Since January 2020 Elsevier has created a COVID-19 resource centre with free information in English and Mandarin on the novel coronavirus COVID-19. The COVID-19 resource centre is hosted on Elsevier Connect, the company's public news and information website.

Computational and Theoretical Chemistry 1217 (2022) 113902

Contents lists available at ScienceDirect

Computational and Theoretical Chemistry

journal homepage: www.elsevier.com/locate/comptc

Trivalent and pentavalent atoms doped boron nitride nanosheets as Favipiravir drug carriers for the treatment of COVID-19 using computational approaches

Afiya Akter Piya *, Tanvir Ahmed, Md. Abdul Khaleque, Kabir Ahmed, Siraj Ud Daula Shamim

Department of Physics, Mawlana Bhashani Science and Technology University, Tangail 1902, Bangladesh

ARTICLE INFO

Keywords:
DFT
COVID-19
Favipiravir
Nanosheets
COSMO
Drug delivery

ABSTRACT

In our DFT investigations, pristine BNNS as well as trivalent and pentavalent atoms doped BNNS have been taken into consideration for Favipiravir (FPV) drug carriers for the treatment of COVID-19. Among the nanosheets, In doped BNNS (BN(In)NS) interacts with FPV by favorable adsorption energies about −2.44 and −2.38 eV in gas and water media respectively. The charge transfer analysis also predicted that a significant amount of charge about 0.202e and 0.27e are transferred to BN(In)NS in gas and water media respectively. HOMO and LUMO energies are greatly affected by the adsorption of FPV on BN(In)NS and energy gap drastically reduced by about 38.80 % and 64.07 % in gas and water media respectively. Similar results are found from the global indices and work function analysis. Therefore, it is clearly seen that dopant In atom greatly modified the BNNS and enhanced the adsorption behavior along with sensitivity, reactivity, polarity towards the FPV.

1. Introduction

Coronavirus (COVID-19) outbreaks have spread worldwide since December 2019, creating a severe public health issue. [1]. The SARS-CoV-2 virus is responsible for COVID-19 disease which infects human instantaneously [2]. Favipiravir (FPV), remdesivir, chloroquine, and lopinavir/ritonavir are some of the antiviral medicines that have been employed in the therapy whereas Favipiravir is an authorized antiviral drug for the treatment of influenza in Japan [2,3]. Chen et al. [4] found that Favipiravir might be an effective medicine against COVID-19 by improving the recovery rate on Day 7. For the first time, Favipiravir was clinically used in China to treat coronavirus illness. In very short period, this disease spreads globally and Favipiravir got approval for emergency use in many countries [5].

Mechanism of Favipiravir drug:

The drug's active form, Favipiravir-RTP goes through phosphoribosylation within the tissue. It reveals its antiviral activity by the following process,

1. The enzyme RNA-dependent RNA-polymerase (RdRp) uses this molecule as a substrate, which misinterprets it as a purine nucleotide [6], blocking its activity and causing viral protein synthesis to stop.
2. It's integrated into the viral RNA strand, stopping it from further extension [7].

Although FPV is approved for emergency use to treat COVID-19 disease, it has some side effects such as teratogenicity, hyperuricemia [8], liver damage and renal injury [9]. To reduce these side effects and increase selectivity, the development of drug delivery systems has been attractive recently [1]. Nanomaterials have been potential candidates for drug delivery purposes to target invaded cells and also control the drug release rate [10]. Different types of nanomaterials including zero-dimensional (0D) nanoclusters, one-dimensional (1D) nanotubes and two-dimensional (2D) nanosheets are used in drug delivery applications [11–14]. Among these nanomaterials, 2D nanosheets have been promising because of their high surface-to-volume ratio, tunable functionalities, high thermal stability and high solubility in biological fluids [15,16]. Chemically, Boron nitride (BN) nanosheets have more stability than graphene [17]. Other properties like high thermal conductivity, excellent mechanical strength, large surface areas, superb oxidation resistance and good chemical inertness make BN nanosheet more attractive [18–20].

BN nanosheet is a promising nanomaterial due to its wide range of applications such as antibacterial agent, anticancer drug delivery [21],

* Corresponding author.
E-mail address: afiya@mbstu.ac.bd (A. Akter Piya).

https://doi.org/10.1016/j.comptc.2022.113902
Received 19 August 2022; Received in revised form 23 September 2022; Accepted 26 September 2022
Available online 30 September 2022

light sensing [22], ultra-microelectrodes [23], field effect transistors (FETs) [24], nanofillers [25] etc. BN nanosheets have been synthesized experimentally by mechanical cleavage [26], ball milling procedure [27], high-energy electron radiation [28] and other several methods [29]. It has been studied widely as a drug carrier by the researchers who found that BN nanosheet is an auspicious candidate for various drugs [30,31]. Additionally, Hilder et al. [32] used molecular dynamic simulation to investigate the interaction of BN nanosheet with cell membranes. Furthermore, BN nanosheet investigated as a drug carrier for cisplatin [13], Doxorubicin [33], Flutamide [34] using DFT. Rakib et al. investigated the adsorption behaviour of metronidazole drug with the boron nitride and boron carbide nanosheets and claimed that BN may be used as drug carrier for metronidazole drug [35]. Another observation suggested that doping of Al, Ga, P and As in the BN nanosheet increase the sensitivity as well as the adsorption behavior [36,37]. In our previous work, we found that doped nanosheets show better adsorption behavior than pristine BN nanosheet when B atoms of BN nannosheet were replaced by Al, Ga and In [38].

In this work, the interaction of FPV with B replaced Al, Ga and In doped BN nanosheets and N replaced P, As and Sb doped BN nanosheets has been investigated by using density functional theory (DFT). We have done different analysis like frontier molecular orbital (FMO), Hirshfeld charge analysis, conductor-like screening model (COSMO) analysis to investigate reactivity and sensitivity of the nanosheet toward FPV drug. All calculations were observed in gas and water phase to analyze the reactivity in both media.

2. Computational details

To investigate the adsorption behavior and geometrical relaxation of FPV drug on nanosheets, DFT was implemented in Dmol3 module. Grimme was selected into dispersion corrected density functional theory (DFT-D) [38]. Generalized gradient approximation (GGA) has better accuracy to predict results for total energy, atomization and energy barrier and the Perdew-Burke-Ernzerhof (PBE) was chosen as a function of GGA to describe the exchange–correlation interaction [39]. Both DFT-D semi-core pseudopotential (DSPP) and double numerical basis set plus polarization (DNP) were set in all calculations for core treatment [40].

The interaction between FPV drug and nanosheets is described by analyzing some parameters such as adsorption energy, interaction distance, energy gap, change in energy gap, charge transfer etc. The adsorption energy (E_{Ad}) has been calculated by the equation given below [41],

$$E_{Ad} = E_{Drug+Nanosheet} - E_{Drug} - E_{Nanosheet} \quad (1)$$

where, $E_{Nanosheet}$ and E_{Drug} are the total energy of nanosheet and drug respectively. $E_{Drug+Nanosheet}$ describes the total energy of complex. Equation (1) illustrates that negative adsorption energy indicates an attractive interaction when drug adsorbs on nanosheet [42]. The Highest Occupied Molecular Orbital (HOMO) and the Lowest Unoccupied Molecular Orbital (LUMO) energies are used to investigate the electronic properties by calculating energy gap. The following equation has been used to measure the energy gap (E_g) [43],

$$E_g = E_{LUMO} - E_{HOMO} \quad (2)$$

where, E_{LUMO} and E_{HOMO} are the energy of LUMO level and the energy of HOMO level respectively. The sensitivity of nanosheet toward drug has been observed by the change in energy gap [44],

$$\Delta E_g = \left[\frac{(E_{g2} - E_{g1})}{E_{g1}}\right] \times 100\% \quad (3)$$

where, E_{g1} and E_{g2} are the energy gap of nanosheet before and after adsorption of drug respectively.

Quantum mechanical descriptors such as chemical potential (μ), hardness (η), softness (S) and electrophilicity index (ω) have been computed to investigate the stability and reactivity. These parameters are calculated by the set of equation as follows [45–47],

$$\text{Chemical potential, } \mu = \frac{(E_{HOMO} + E_{LUMO})}{2} \quad (4)$$

$$\text{Global hardness, } \eta = \frac{(E_{LUMO} - E_{HOMO})}{2} \quad (5)$$

$$\text{Softness, } S = \frac{1}{2\eta} \quad (6)$$

$$\text{Global electrophilicity, } \omega = \frac{\mu^2}{2\eta} \quad (7)$$

The amount of transferred charge between nanosheet and drug has also been studied. Electrostatic potential (ESP) map shows the positively charged region and negatively charged region. Since FPV drug is used for human being and the common transportation medium in human body is liquid, all calculations have also been conducted in solvation media alongside the gas phase. The conductor-like screening model (COSMO) method is introduced to analyze the solvation effect on complexes [48–50].

3. Results and discussion

3.1. Nanosheets and FPV drug

In our investigation, pristine boron nitride nanosheet (BNNS) and trivalent (Al, Ga and In) and pentavalent (P, As and Sb) atoms doped BNNS have been taken into consideration as drug carrier for FPV drug molecule [10,51,52]. A 12x18 Å dimensions of BNNS has been chosen with 16 hexagons where hydrogen atoms are used as terminal atom due to stability purpose. After geometry optimization, 1.44, 1.20 and 1.01 Å bond distances are found for B–N, B–H and N—H which are consistent with previous study [35]. To enhance the adsorption performance of the BNNS, we have modified BNNS by doping trivalent (Al, Ga and In) atoms in the place of central B atom and by pentavalent (P, As and Sb) atoms in the place of central N atom. All nanosheets are further optimized and shown in Fig. 1. After optimization, all nanosheets remain in planer form where the bond distances are varied at the dopant site. The bond distances between the dopant Al, Ga, In, P, As and Sb atoms and their neighboring atoms are 1.72, 1.74, 1.90, 1.75, 1.80 and 1.94 Å in BN(Al)NS, BN(Ga)NS, BN(In)NS, BN(P)NS, BN(As)NS and BN(Sb)NS respectively. The optimized FPV drug with HOMO, LUMO and ESP maps are shown in Fig. 2. It contains three C—C bonds with an average bond distance of about 1.445 Å, five C—N bonds of 1.337 Å, two C—O bonds of 1.29 Å, one C-F bond of 1.357 Å, two N—H bonds of 1.015 Å, one C—H bond of 1.091 Å and one O—H bond of 0.98 Å. Our calculated average bond lengths are in good agreement with previous experimental values which are 1.48 Å for C—C, 1.32 Å for C—N, 1.31 Å for C—O, 1.34 Å for C-F bonds [53]. The HOMO levels of FPV drug are mostly located on the C—O bond and LUMO levels are mostly concentrated on the C—C and C—N bonds.

3.2. Interaction of FPV on the B replaced by Al, Ga and in doped BNNS

Initially different adsorption configurations have been tested to find suitable adsorption position of FPV drug molecule on the nanosheets. High interaction energy with stable configuration is found, when FPV drug molecule is adsorbed in a parallel position to the BNNS. Therefore, all calculations have been performed by taking FPV drug molecule on the BNNS in parallel configuration. First of all, all the complexes are optimized in ground state and illustrated in Fig. 3. In our optimized complexes, nanosheets are deformed in the defected site where the dopant atoms are displaced towards the FPV drug due to large atomic

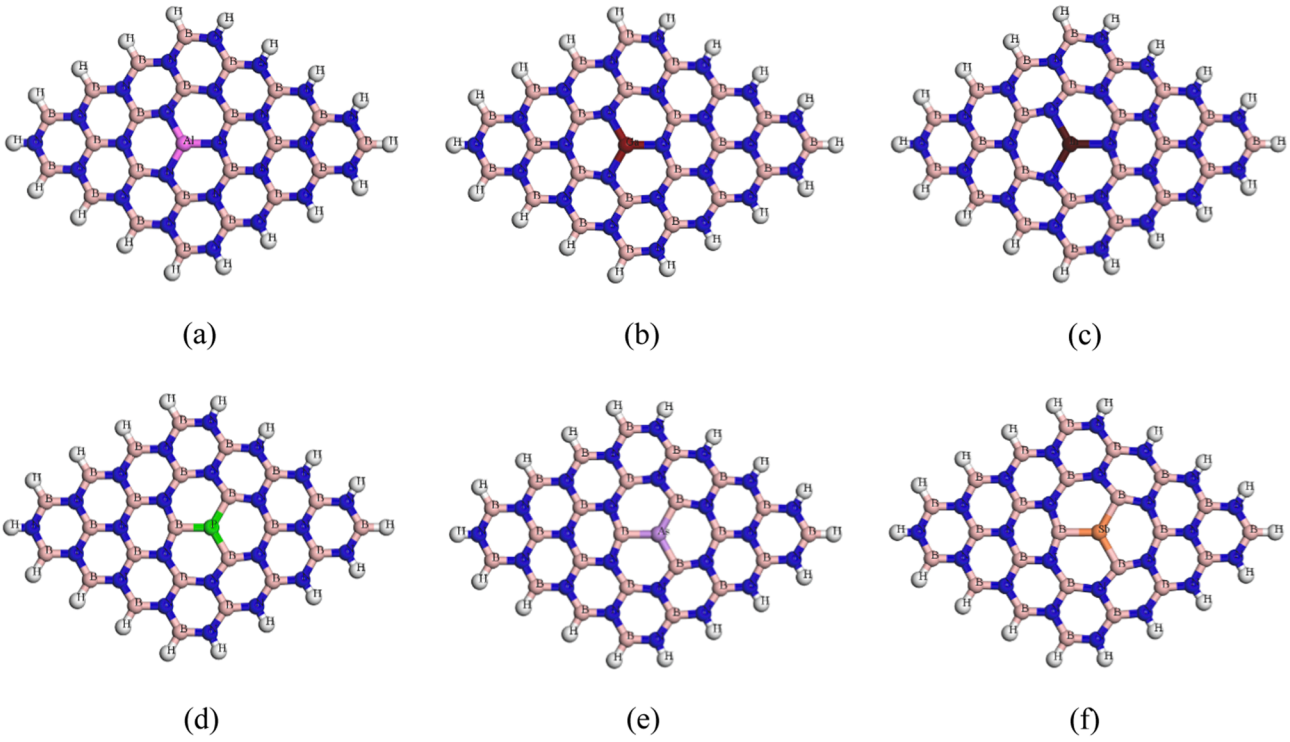

Fig. 1. Optimized structures of (a) BN(Al)NS, (b) BN(Ga)NS, (c) BN(In)NS, (d) BN(P)NS, (e) BN(As)NS, (f) BN(Sb)NS respectively.

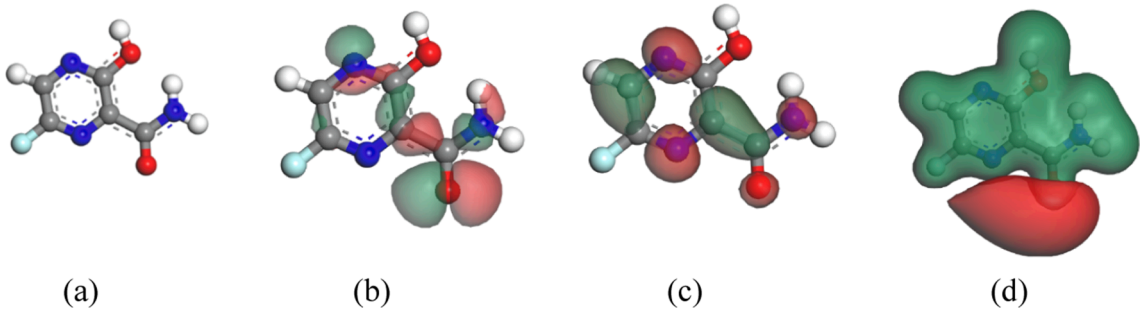

Fig. 2. (a) Optimized structure, (b) HOMO, (c) LUMO and (d) ESP maps of Favipiravir drug.

radius of dopant atoms and high interaction energies. Among the Al, Ga and In dopant atoms, In atom is highly displaced to the FPV drug and the drug is also slightly deformed. The adsorption energies have been investigated and reported in Table 1. In case of intrinsic BNNS, the low interaction energy has been found which is −0.70 eV. FPV adsorbs on BNNS by keeping a large interaction distance of 3.43 Å. Negative adsorption energy implies the attractive and exothermic reaction where below −0.8 eV indicates the physisorption interaction and above the value of −0.8 eV indicates the chemisorption interaction between drug and nanosheets [54]. During the adsorption process, FPV losses a small amount of charge of about 0.055e to the nanosheet according to Hirshfeld charge analysis. As BNNS shows less adsorption behavior towards the FPV drug, we have modified the BNNS by doping Al, Ga and In atom in the position of center B atom of BNNS to improve the sensitivity of the BNNS as previously mentioned. After doping Al and Ga atoms on the BNNS, the interaction energies slightly improved which are about −0.88 and −0.86 eV, by transferring 0.172e and 0.072e amount of charge from FPV to BN(Al)NS and BN(Ga)NS respectively. The minimum interaction distances are 2.70 and 3.06 Å for BN(Al)NS and BN(Ga)NS respectively. But in case of adsorption of FPV on the In doped BNNS, the interaction energy greatly enhanced to about −2.44 eV by transferring significant amount of charge of about 0.202e from FPV to BN(In)NS. Therefore, In doped BNNS shows high sensitivity towards the FPV drug molecule.

The most valuable parts of the human body such as the heart, lungs and kidneys are composed of 73 %, 83 % and 79 % water. Therefore, the solvation effect on our complexes are also examined in the solvent media like water media. The adsorption phenomenon is also investigated in the water media and the adsorption energy values with adsorption distance and charge transfer are shown in Table 1. The adsorption behavior is slightly reduced in water media due to presence of water molecules in the interaction point to resist the direct contact between drug and nanosheets. The calculated adsorption energies are −0.81, −0.71 and −2.38 eV for FPV/BN(Al)NS, FPV/BN(Ga)NS and FPV/BN(In)NS respectively. During the interaction between FPV with the nanosheets, 0.225e, 0.086e and 0.27e amounts of charge are transferred to the BN(Al)NS, BN(Ga)NS and BN(In)NS respectively. Therefore, it is clearly seen that FPV drug interacts with In doped BNNS by high interaction energy and transferring a significant amount of charge in both gas and water media.

3.3. Interaction of FPV on the N replaced P, As and Sb doped BNNS

In our previous section, we have discussed about Al, Ga and In doped

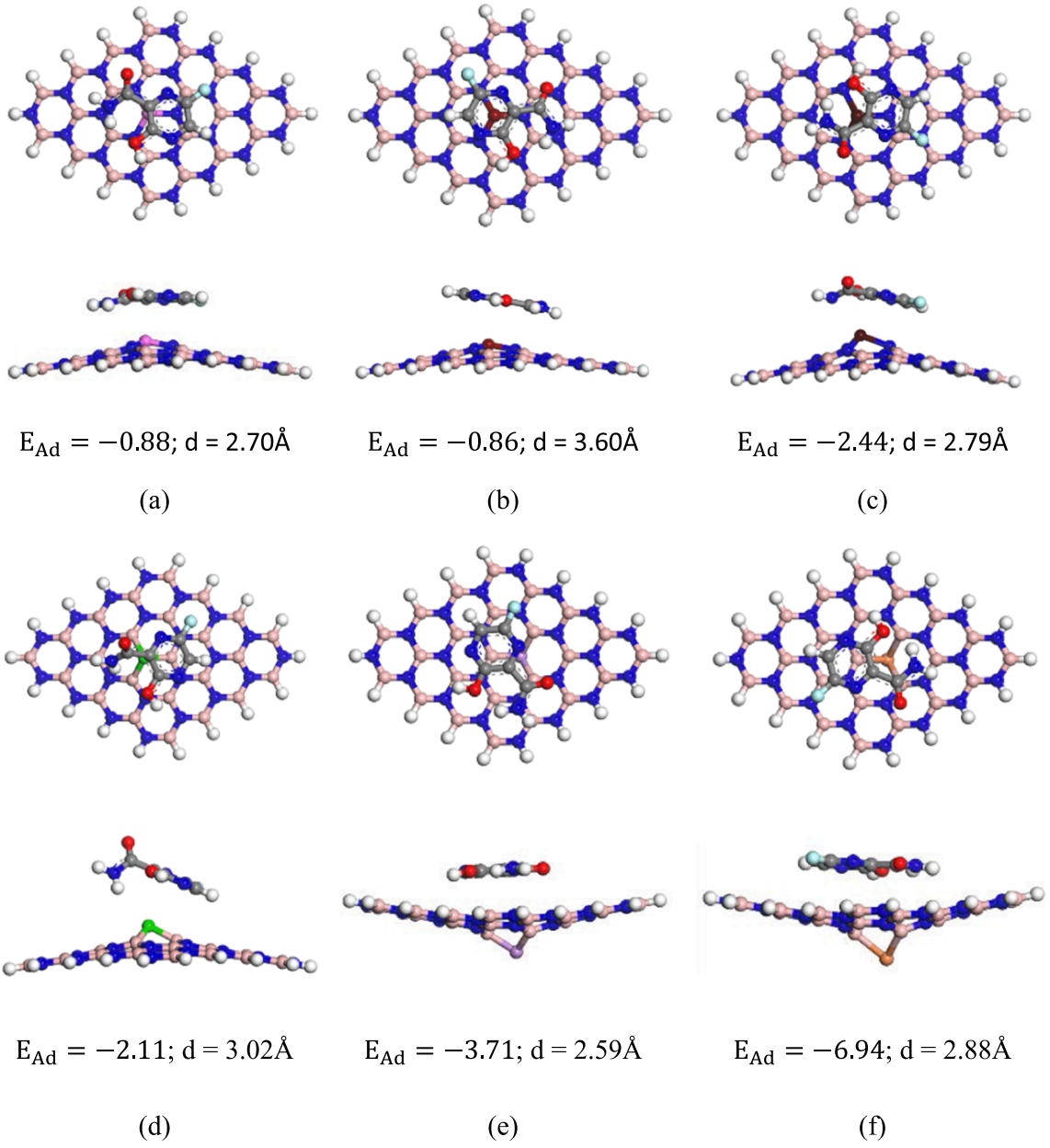

Fig. 3. Optimized geometries of (a) FPV/BN(Al)NS (b) FPV/BN(Ga)NS, (c) FPV/BN(In)NS, (d) FPV/BN(P)NS, (e) FPV/BN(As)NS and (f) FPV/BN(Sb)NS complexes respectively.

Table 1
The calculated minimum interaction distance (d) in Å, adsorption energy (E_{Ad}) in eV and charge transfer (ΔQ) in e between Favipiravir and nanosheets in both gas and water phases.

Structure	Gas Phase			Water Phase		
	d	E_{Ad}	ΔQ	d	E_{Ad}	ΔQ
FPV/BNNS	3.43	−0.70	0.055	3.43	−1.23	0.053
FPV/BN(Al)NS	2.70	−0.88	0.172	2.58	−0.81	0.225
FPV/BN(Ga)NS	3.06	−0.86	0.072	3.05	−0.71	0.086
FPV/BN(In)NS	2.79	−2.44	0.202	2.67	−2.38	0.27
FPV/BN(P)NS	3.02	−2.11	−0.050	3.14	−0.66	−0.04
FPV/BN(As)NS	2.59	−3.71	0.031	2.70	−3.46	0.04
FPV/BN(Sb)NS	2.88	−6.94	0.032	2.96	−6.65	0.03

BNNS in the place of center B atom and it is found that In doped BNNS shows high sensitivity for FPV drug. Now in this section, we will discussed about the interaction behavior of P, As and Sb doped BNNS towards FPV drug. The adsorption energies have been found to be −2.11, −3.71 and −6.94 eV for P, As and Sb doped BNNS respectively. Thus, P, As and Sb doped BNNS show high interaction stability towards the FPV drug than Al, Ga and In doped BNNS. During the interaction between FPV and BN(P)NS, dopant P atom displaces upward out of sheet towards the FPV indicating that interaction takes place between the dopant P atom and FPV drug. But in case of BN(As)NS and BN(Sb)NS, the dopant atoms displace downward out of sheets. The FPV adsorbs on the P, As and Sb doped BNNS by maintaining 3.02, 2.59 and 2.88 Å adsorption distances. During the interaction, FPV drug gains 0.05e charge from BN(P)NS but in case of BN(As)NS and BN(Sb)NS, FPV drug losses 0.031e and 0.032e amount of charge to the nanosheets respectively. In the water solvent media, the interaction energies are found to be −0.66, −3.46 and −6.65 eV for BN(P)NS, BN(As)NS and BN(Sb)NS respectively. A very poor amount of charges are transferred between the FPV and the nanosheets in the water media in the range of 0.03e ~ 0.04e. A comparison of adsorption energies of different nanosheets in

both gas and water phases is shown in Fig. 4. We can see from Fig. 4 that adsorption energy is increased in water media compared with the gas phase for BNNS. But for other nanosheets, the values of adsorption energy tend to go downward in water media than gas phase.

3.4. Frontier molecular orbital (FMO) analysis

Frontier molecular orbital (FMO) analysis such as HOMO energies, LUMO energies and energy gap have been studied to explore the sensitivity of the FPV drug towards the nanosheets and the calculated values are reported in Table 2. The HOMO and LUMO maps with electrostatic potential (ESP) map of the complexes are shown in Fig. 5. It is seen that the HOMO levels are situated on the nanosheets except P doped BNNS and LUMO levels are located on the FPV drug molecule. HOMO levels of Al, Ga and In doped BNNS are found at −5.85, −5.87 and −5.87 eV respectively. After adsorption of FPV on the nanosheets, the HOMO energies are slightly shifted to higher energy values to −5.78, −5.80 and −5.67 eV. But in case of LUMO energies, energy values are highly reduced from −1.48 to −3.87, −1.50 to −3.50 and −1.54 to −4.14 eV indicating the high reduction of energy gaps. The energy gap "E_g" is determined from the differences between the LUMO and HOMO energies. The obtained energy gaps are 4.38, 4.37, 4.37, 4.33, 3.45, 3.14 and 2.59 eV of BNNS, BN(Al)NS, BN(Ga)NS, BN(In)NS, BN(P)NS, BN(As)NS and BN(Sb)NS respectively. But after the adsorption of FPV drug on the nanosheets, the energy gaps are greatly reduced to 2.64, 1.91, 2.30, 2.65, 2.91, 2.55 and 2.29 eV respectively. The reduction of energy gap indicates the increasing sensitivity of the nanosheets towards the FPV drug molecule and it leads to exponential increment of conduction electron density found by the following equation. The energy gap of nanosheets reduced due to the interaction of drug molecule which is investigated by density of states (DOS). Fig. 6 shows the DOS spectra of nanosheets before and after the adsorption process. The conduction electron density (N) depends on the E_g related to the following relation [55],

$$N = AT^{3/2}e^{\left(\frac{-E_g}{2KT}\right)} \quad (8)$$

where, K is the Boltzmann's constant = $1.380 \times 10^{-23}\ m^2kgs^{-2}k^{-1}$ and A (electrons/$m^3/k^{3/2}$) is a constant.

The calculated percentage of reduction in energy gap (%E_g) for Al, Ga and In doped BNNS are found to be 56.29 %, 47.26 % and 64.84 % respectively. On the other hand, for P, As and Sb doped BNNS, the reduction in energy gaps are about 15.65 %, 18.79 % and 11.58 % respectively. The comparison of energy gap between different

Table 2
HOMO energies (E_{HOMO}), LUMO energies (E_{LUMO}), HOMO-LUMO energy gap (E_g) in eV and change in energy gap (%ΔE_g) in gas phase.

Structure	E_{HOMO}	E_{LUMO}	E_g	%ΔE_g
FPV	−6.01	−3.36	2.65	–
BNNS	−5.84	−1.46	4.38	
FPV/BNNS	−5.78	−3.15	2.64	39.85
BN(Al)NS	−5.85	−1.48	4.37	
FPV/BN(Al)NS	−5.78	−3.87	1.91	56.29
BN(Ga)NS	−5.87	−1.50	4.37	–
FPV/BN(Ga)NS	−5.80	−3.50	2.30	47.26
BN(In)NS	−5.87	−1.54	4.33	–
FPV/BN(In)NS	−5.67	−4.14	2.65	38.80
BN(P)NS	−4.98	−1.53	3.45	–
FPV/BN(P)NS	−5.68	−2.77	2.91	15.65
BN(As)NS	−4.68	−1.54	3.14	–
FPV/BN(As)NS	−5.72	−3.17	2.55	18.79
BN(Sb)NS	−4.17	−1.59	2.59	–
FPV/BN(Sb)NS	−5.48	−3.19	2.29	11.58

Table 3
Computed chemical potential (μ), global hardness (η), electrophilicity index (ω) and global softness (S) of the studied complexes in gas phase.

Structure	μ	η	ω	S
FPV	−4.68	1.32	8.29	0.38
BNNS	−3.65	2.19	3.04	0.23
FPV/BNNS	−4.47	1.32	7.56	0.38
BN(Al)NS	−3.67	2.19	3.08	0.23
FPV/BN(Al)NS	−4.82	0.96	12.18	0.52
BN(Ga)NS	−3.68	2.18	3.10	0.23
FPV/BN(Ga)NS	−4.64	1.52	9.36	0.43
BN(In)NS	−3.71	2.17	3.17	0.23
FPV/BN(In)NS	−4.90	0.76	15.77	0.66
BN(P)NS	−3.26	1.73	3.07	0.29
FPV/BN(P)NS	−4.23	1.46	6.13	0.34
BN(As)NS	−3.11	1.57	3.08	0.32
FPV/BN(As)NS	−4.45	1.28	7.75	0.39
BN(Sb)NS	−2.88	1.29	3.21	0.39
FPV/BN(Sb)NS	−4.34	1.15	8.21	0.44

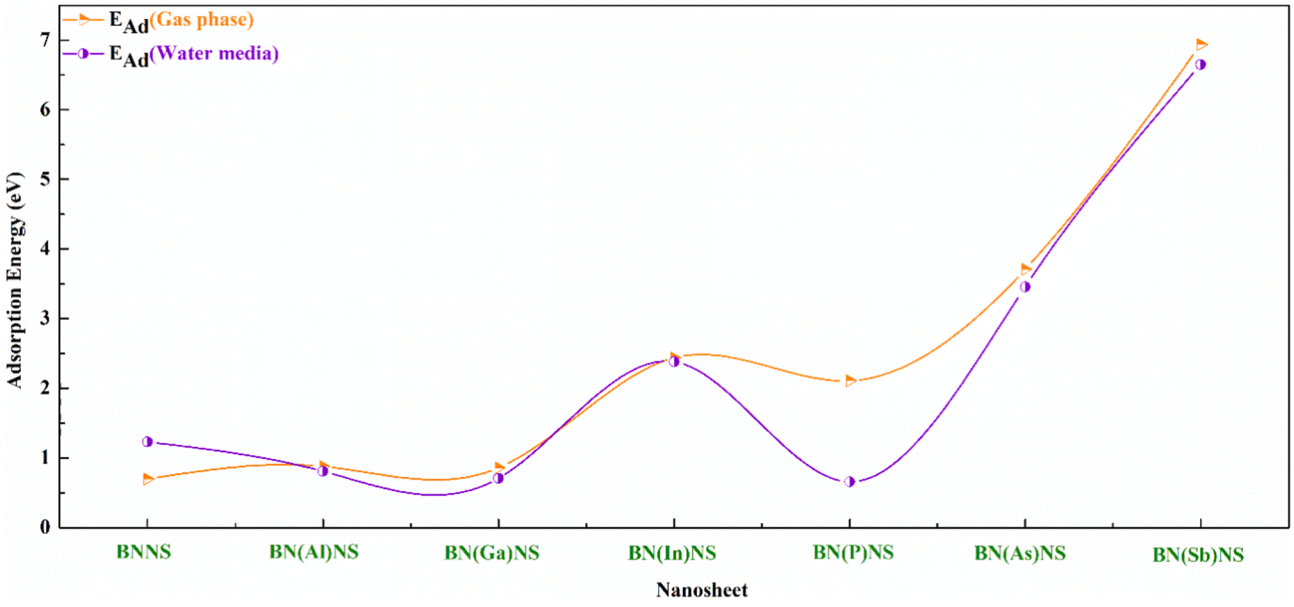

Fig. 4. A comparison of adsorption energies of different nanosheets in both gas and water phase.

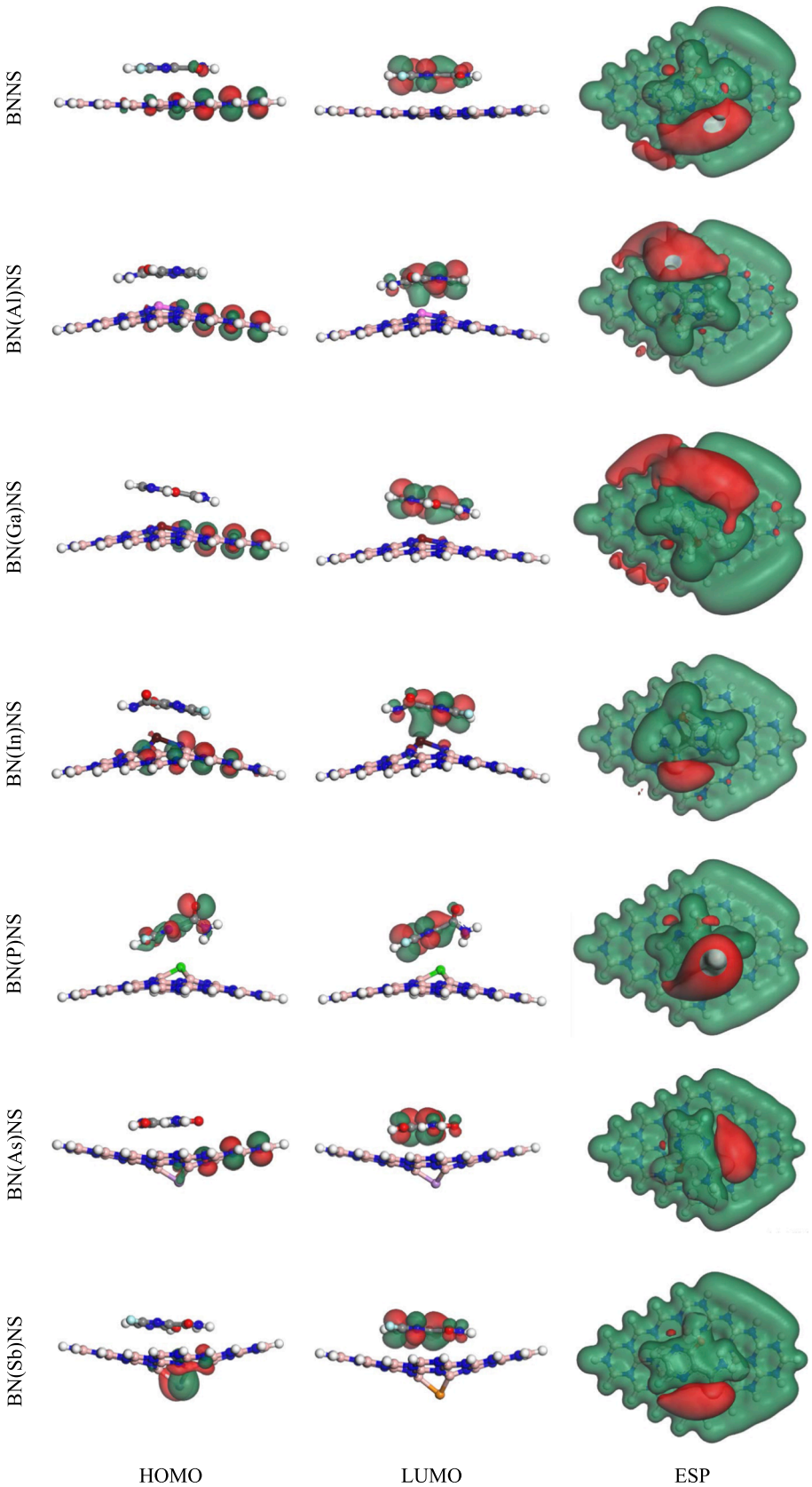

Fig. 5. HOMO, LUMO and ESP maps of the complexes.

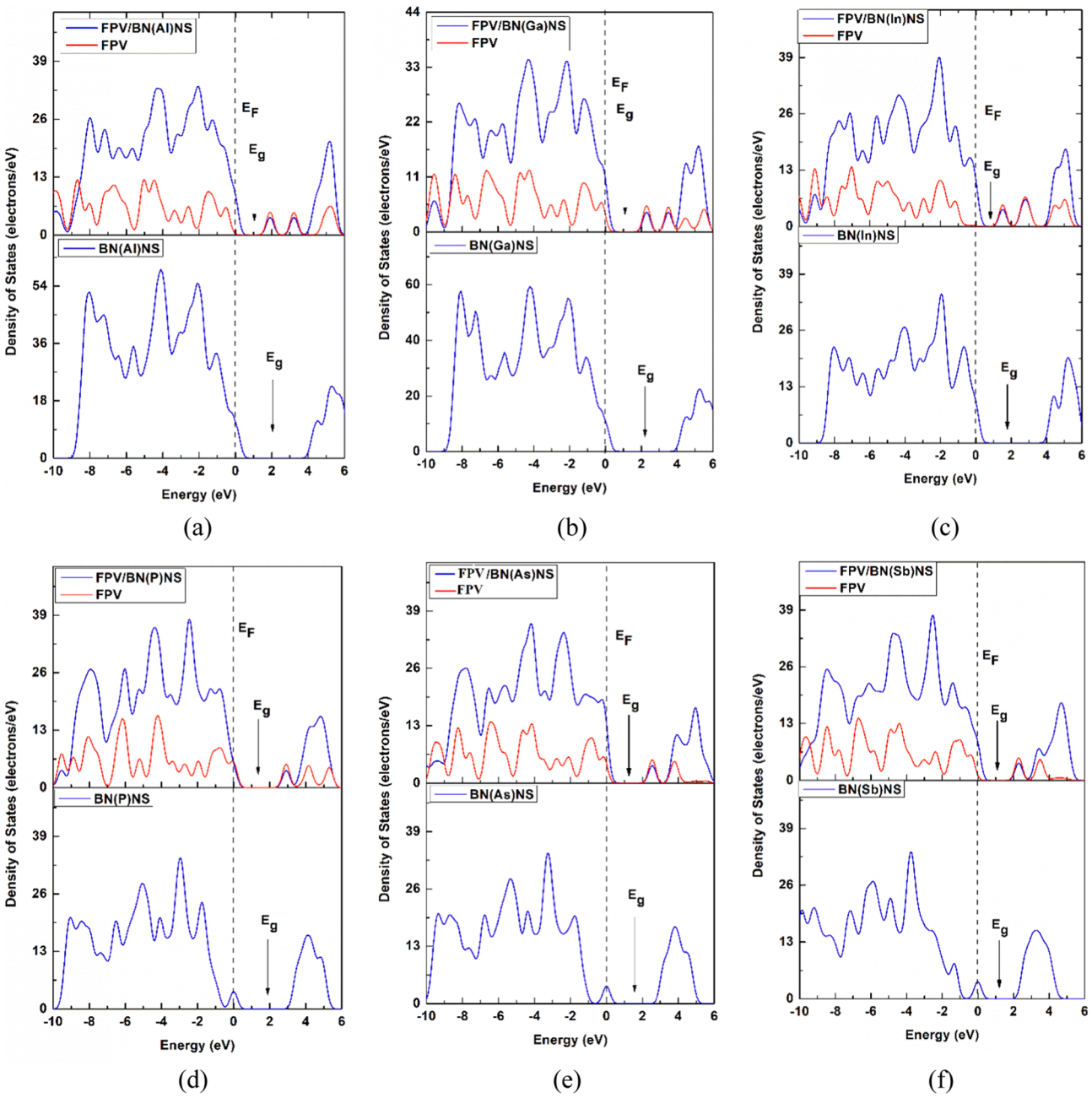

Fig. 6. The total and partial DOS of (a) BN(Al)NS (b) BN(Ga)NS, (c) BN(In)NS, (d) BN(P)NS, (e) BN(As)NS and (f) BN(Sb)NS before and after adsorption of FPV drug. The dotted line indicates the Fermi level.

nanosheets and complexes is drawn in Fig. 7. In comparison with pentavalent (P, As and Sb) doped BNNS, trivalent (Al, Ga and In) doped BNNS show more sensitivity towards the FPV drug. Higher the reduction of energy gap implies the higher sensitive nanosheet with the drug molecule. Sensor response factor R is also observed which exponentially depends on the change in energy gap as follows [56],

$$R = \frac{\sigma_1}{\sigma_2} = exp(-\frac{\Delta E_g}{2kT}) \quad (9)$$

where, σ_1 and σ_2 are the electrical conductivity signals related to the nanosheets and the complexes respectively. From the equation, it is clearly seen that the Al and In doped BNNS is more sensitive towards the FPV drug.

3.5. Dipole moment

Dipole moment is a vital parameter which predicts the polar nature of the chemical bond. When the center of positive and center of negative charges are not coincided at the same point in a molecule then the polar nature of molecule is raised. Zero value of dipole moment indicates the non-polar nature of molecule [49]. With the increasing dipole moment, the polar nature of the chemical bond is increased. The values of dipole moment are reported in Table 4. In our studied drug, the dipole moment is found to be 5.69 and 8.27 D in gas as well as water media. FPV drug shows the polarity, which means an asymmetric charge distribution occurred in the molecule. The polarity of the FPV is enhanced in the water media. BNNS also shows polarity with dipole moment of about 5.78 D and 6.10 D in gas and water media respectively. After doping Al, Ga and In atom on the BNNS, the dipole moment slightly enhances to

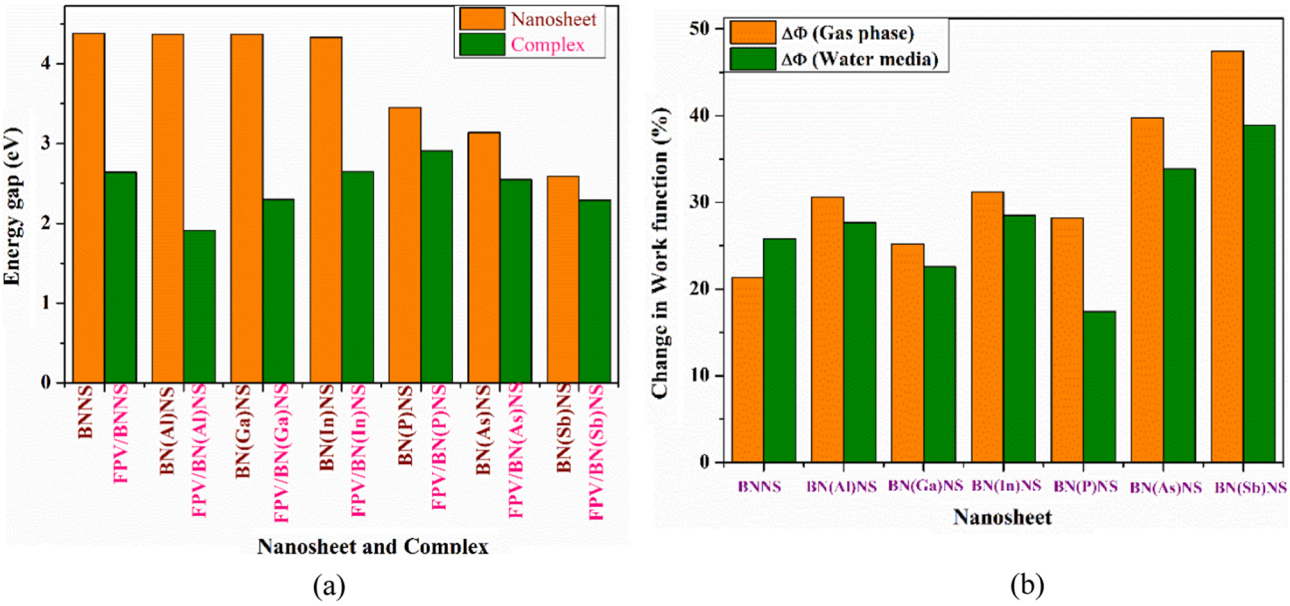

Fig. 7. Comparison of the (a) energy gap and (b) change in work function between different nanosheets and complexes.

Table 4
Fermi level energies (E_F), work function (φ) and change in work function (% φ) for the studied complexes in both gas phase and water phases.

Structure	Gas phase				Water phase			
	E_F(eV)	φ (eV)	%φ	D.M	E_F(eV)	φ (eV)	%φ	D.M
FPV	−4.68	4.68	–	5.69	−4.86	4.86	–	8.27
BNNS	−3.64	3.64	–	5.78	−3.64	3.64	–	6.10
FPV/BNNS	−4.42	4.42	21.37	6.31	−4.58	4.58	25.76	10.27
BN(Al)NS	−3.66	3.66	–	5.95	−3.82	3.82	–	8.25
FPV/BN(Al)NS	−4.78	4.78	30.59	7.02	−4.87	4.87	27.66	11.03
BN(Ga)NS	−3.67	3.67	–	5.98	−3.82	3.82	–	8.29
FPV/ BN(Ga)NS	−4.60	4.60	25.21	6.25	−4.69	4.69	22.59	10.33
BN(In)NS	−3.70	3.70	–	6.07	−3.84	3.84	–	6.42
FPV/ BN(In)NS	−4.86	4.86	31.20	7.34	−4.94	4.94	28.51	12.40
BN(P)NS	−3.28	3.28	–	6.03	−3.57	3.57	–	8.39
FPV/BN(P)NS	−4.21	4.21	28.21	9.09	−4.19	4.19	17.42	9.59
BN(As)NS	−3.14	3.14	–	6.10	−3.44	3.44	–	8.50
FPV/BN(As)NS	−4.39	4.39	39.78	2.45	−4.60	4.60	33.89	3.96
BN(Sb)NS	−2.91	2.91	–	6.24	−3.24	3.24	–	8.75
FPV/BN(Sb)NS	−4.30	4.30	47.42	7.02	−4.49	4.49	38.91	11.48

5.95, 5.98 and 6.07 D in gas phase and 8.25, 8.29 and 6.42 D in water media which indicates that all our proposed nanosheets show polar nature in gas phase and water media also. After adsorption of FPV drug on the polar nanosheets, the polarity further enhances i.e., for BNNS and Al, Ga and In doped BNNS, the dipole moments are 6.31, 7.02, 6.25 and 7.34 D in gas phase and 10.27, 11.03, 10.33 and 12.40 D in water media respectively. Similar phenomenon is found in case of P, As and Sb doped BNNS. Therefore, after adsorption of FPV drug on the nanosheets, the asymmetricity of the complexes are increased due to transferring of charge between the drug and nanosheets. In our charge transfer analysis, it is found that as Al and In doped BNNS transfer large amount of charge with the FPV, the dipole moments of the complexes are high enough among the others. In our study, it is clearly found that the dipole moments of the complexes are higher in water media than gas media which means the solubility of the complexes is increased in polar media like water media.

3.6. Quantum molecular descriptors

Quantum molecular descriptors (QMD) such as chemical potential (μ), global hardness (η), global softness (S) and electrophilicity index (ω) have been investigated to analyze the reactivity of our nanosheets towards the FPV drug. The values are presented in Table 3. In drug delivery purposes, it is desired to increase the chemical potential, global softness and electrophilicity after adsorption of drug molecule [57]. On the contrary, decreasing global hardness is also necessary. In our investigation, we have found the increasing phenomenon of chemical potential, global softness and electrophilicity and decreasing phenomenon of global hardness of our nanosheets during interaction with FPV drug which are displayed in Fig. 8 (a-c). The values of chemical potential of BNNS and Al, Ga and In doped BNNS are –3.65, –3.67, –3.68 and –3.71 eV respectively. After the adsorption of FPV drug, the values of chemical potential are increased to –4.47, –4.82, –4.64 and –4.90 eV respectively. Similarly, for P, As and Sb doped BNNS, the values of chemical potential are enhanced from −3.26 to −4.23, −3.11 to −4.45 and −2.88 to −4.34 eV respectively after the adsorption of FPV drug. Global hardness of BNNS and Al, Ga and In doped BNNS are almost similar which ranges from ~ 2.17 to 2.19 eV but during interaction with FPV, the values are significantly decreased to 1.32, 0.96, 1.52 and 0.76 eV respectively. In case of P, As and Sb doped BNNS, similar phenomenon has been occurred where the values are shifted from 1.73 to 1.46, 1.57 to 1.28 and 1.29 to 1.15 eV respectively. In Table 3, it is clearly seen that there was an increasing tendency of global softness and electrophilicity. These parameters predict that all nanosheets show reactivity

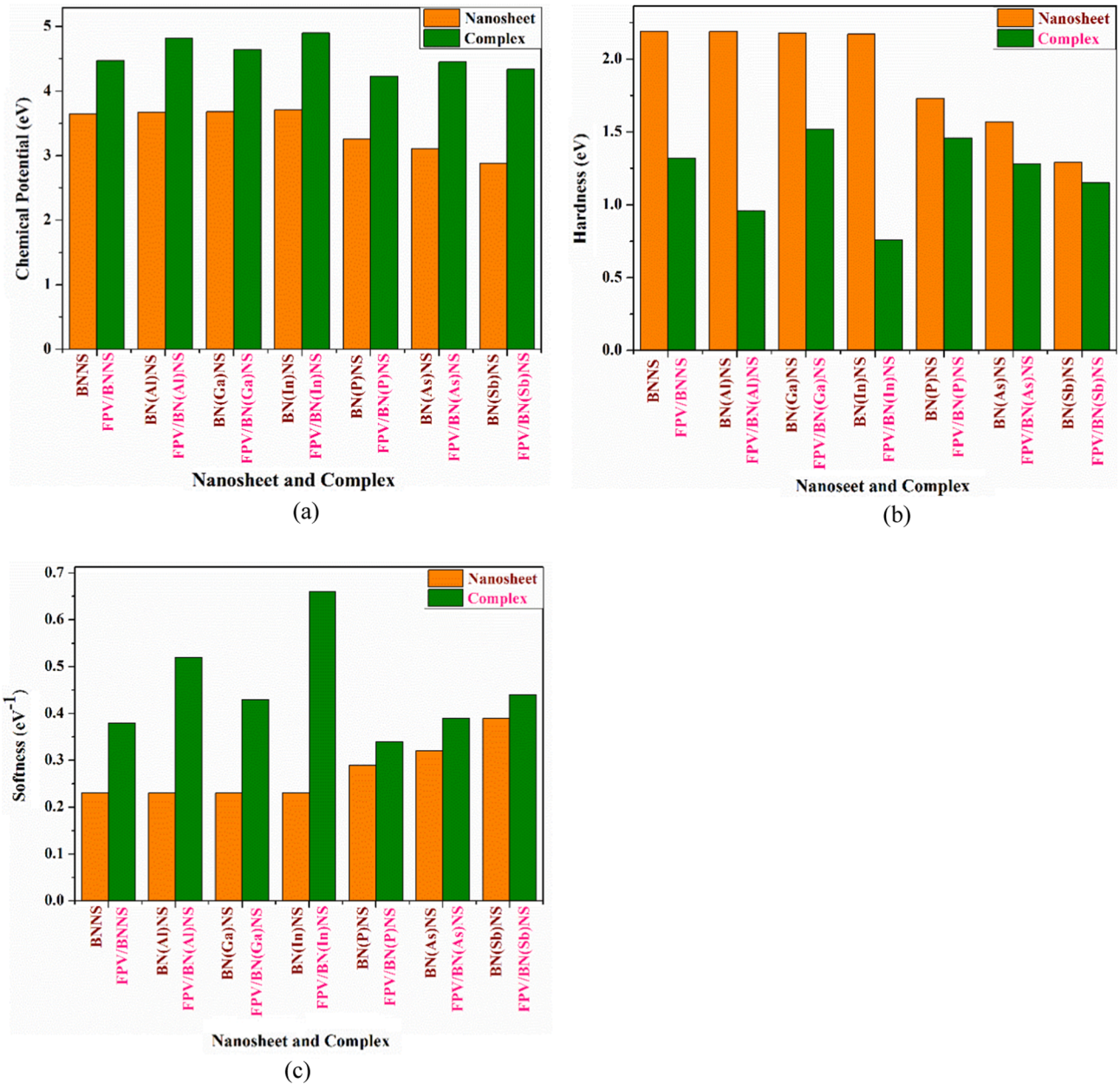

Fig. 8. Comparison of (a) chemical potential, (b) Hardness and (c) Softness between nanosheets and complexes.

towards the FPV drug. But among the nanosheets, Al and In doped BNNS show high reactivity for FPV drug which is consistent with adsorption energy, HOMO and LUMO energies.

3.7. Work function

Work function (φ) is another vital investigation for drug sensing which has been studied. If the FPV drug is affecting the work function of the nanosheets, it affects the gate voltage which produces an electrical signal, helping the chemical recognition. By definition, work function is assume to be the minimum energy required to remove an electron from a solid surface to vacuum instantaneously and defined as follows [13],

$$\varphi = V_{e(+\infty)} - E_F \tag{10}$$

where, E_F and φ correspond to the Fermi level and work function, $V_{e(+\infty)}$ is the electrostatic potential of an electron distant from the surface which we can consider to be zero i.e., $V_{e(+\infty)} = 0$. Hence, the work function is numerically equal to the Fermi level energy, $\varphi = -E_f$.

The field emission characteristics of the nanosheet are altered by varying work function which may consequently end up in changing the gate voltage. This is well explained by the Richardson-Dushman equation [58],

$$j = AT^2 e^{(-\varphi/kT)} \tag{11}$$

j = electron current density emitted from the surface of a material.
K = Boltzmann constant.
T = Temperature.
A = Richardson constant (A/m^2).

The change of work function after adsorption can be calculated by the following formula [59]:

$$\Delta\varphi = \frac{\varphi_f - \varphi_i}{\varphi_i} \times 100\% \tag{12}$$

where, φ_i = initial work function of nanosheets (before adsorption).
φ_f = final work function of nanosheets (after adsorption of drug

molecule).

Table 4 illustrates the computed work functions in gas as well as water media and also shows the change in work functions after adsorption of FPV drug. In our observation, the work function of the nanosheets such as BNNS and Al, Ga and In doped BNNS are 3.64, 3.66, 3.67 and 3.70 eV but after adsorption of FPV drug on the nanosheets, the work functions are shifted to 4.42, 4.78, 4.60 and 4.86 eV. That is, the work functions are changed by 21.37 %, 30.59 %, 25.21 % and 31.20 % respectively. On the other hand, the pentavalent doped (P, As and Sb) BNNS, the change in work functions have been found about 28.21 %, 39.78 % and 47.42 % respectively. Therefore, the doped nanosheets show high change in work function which enhance the chemical recognition during adsorption process. In the solvent media like water media, the change in work functions slightly reduce with respect to gas media except BNNS. The comparison of the change in work function (% φ) between gas and water phases is shown in Fig. 7.

3.8. Solvation effect

It has been earlier mentioned that the solvation effect has been performed for investigating the effect of solvent media like water of dielectric constant 78.54 by employing the conductor-like screening model (COSMO) method on the complexes [60]. Since the human body is mainly made of water, it is essential to investigate the adsorption behavior with solubility of FPV drug on the nanosheets in water solvent media. The adsorption behavior, solubility and work function of FPV drug on the nanosheets in the water media has been discussed previously. In this section, solvation energy with COSMO surface of the complexes will be discussed.

To search the stability of the complexes in the water media, we have calculated solvation energy of the complexes by using the following equation [57],

$$E_{sol} = E_{water} - E_{gas} \quad (13)$$

Where E_{water} is the total energy of the complexes in the water media and E_{gas} is the total energy of the complexes in the gas media. The stability of complexes in the aqueous medium is confirmed by the negative value of solvation energy [61]. Our calculated solvation energy for all complexes are negative values which are −1.19, −1.32, −1.27, −1.40, −1.31, −1.18 and −1.13 eV for BNNS and Al, Ga, In, P, As and Sb doped BNNS with FPV complexes respectively. Among the calculated values, Al and In doped BNNS shows high solvation energy which means that these two complexes show more stability in the water media.

COSMO surface investigation has been performed to get more insight into the solvent effect on the complexes [38]. The polar nature of our complexes has been confirmed by the dipole moment analysis where we found that all the complexes show high polarity in the water media. To visualize the polarity of the complexes, we further analyze the COSMO surface of the complexes which indicates the different polar region of the complexes in water solvent media (Fig. 9). In Fig. 9, red segment implies the negative region of polarity whereas blue segment indicates the positive region of polarity. And the green region means the non-polar portion of the complex. It is clearly seen that all complexes contain the negative and positive portion on the surface which confirm the polarity of the complexes.

4. Conclusions

Favipiravir is one of the most effective antiviral drug which plays an important role in the treatment of COVID-19. To overcome the difficulties such as side effects, mechanism of actions etc. of Favipiravir, nanotechnology can be used to deliver the FPV drug. In our investigation, some promising nanomaterials which are pristine BNNS and trivalent (Al, Ga and In) and pentavalent (P, As and Sb) atoms doped BNNS have been taken into consideration for drug carriers for the treatment of COVID-19. All calculations have been carried out by taking GGA-PBE functional in DFT. Our adsorption energy analysis suggested that all nanosheets are displayed an attractive interaction with FPV drug. But among the nanosheets In doped BNNS shows more adsorption behavior i.e., FPV interacts with BN(In)NS in a favorable range of

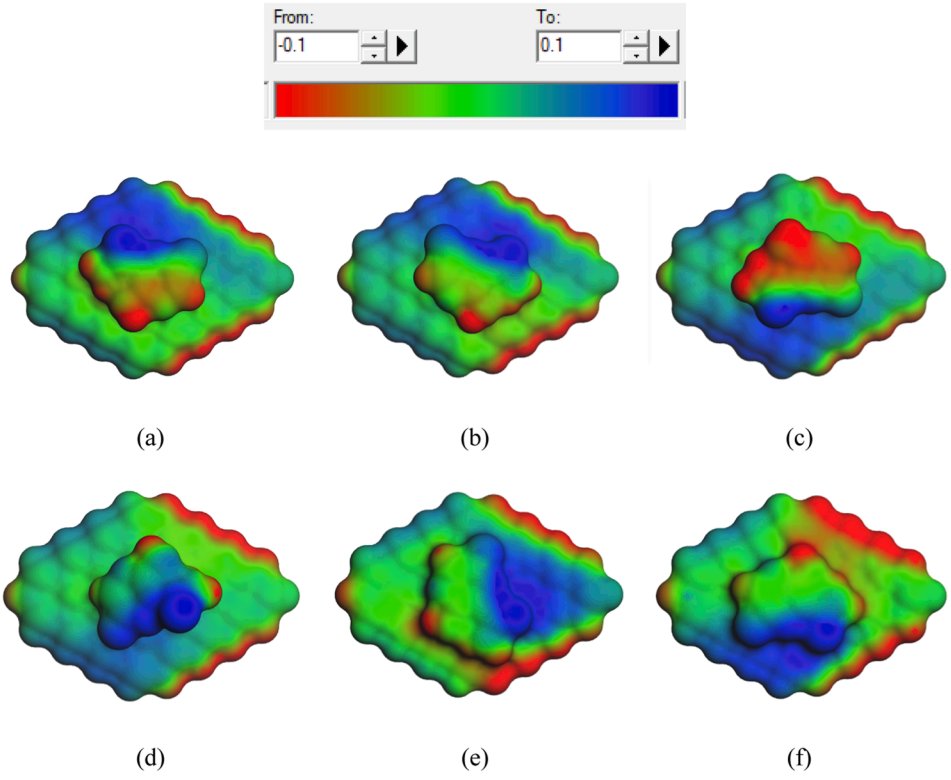

Fig. 9. COSMO surface of (a) FPV/BN(Al)NS (b) FPV/BN(Ga)NS, (c) FPV/BN(In)NS, (d) FPV/BN(P)NS, (e) FPV/BN(As)NS and (f) FPV/BN(Sb)NS complexes.

interaction energy with transferring significant amount of charge. It is found that FPV adsorbs on BN(In)NS by −2.44 and −2.38 eV adsorption energies with transferring the amount of charges of about 0.202e and 0.27e to the nanosheet in both media. The frontier molecular orbital analysis proposed that the HOMO and LUMO energies are greatly affected by the adsorption of FPV drug on the In doped BNNS. Energy gap drastically reduces by about 38.30 % in gas media and 64.07 % in water media which confirms the highest sensitivity. Similar results are found from the global indices and work function analysis in which 31.2 % and 28.51 % of change in work function have been found in gas and water media. Dipole moment and COSMO surface analysis show that in water solvent media, the FPV/BN(In)NS complex show high polarity in the presence of water media which is 12.4 Debye. Therefore, from the above analysis it is clearly seen that dopant In atom greatly modifies the BNNS and enhances the adsorption behavior along with sensitivity, reactivity, polarity etc. towards the FPV drug.

CRediT authorship contribution statement

Afiya Akter Piya: Writing – original draft, Data curation. **Tanvir Ahmed:** Writing – review & editing. **Md. Abdul Khaleque:** Data curation. **Kabir Ahmed:** Data curation. **Siraj Ud Duala Shamim:** Conceptualization, Formal analysis, Supervision.

Declaration of Competing Interest

The authors declare that they have no known competing financial interests or personal relationships that could have appeared to influence the work reported in this paper.

Data availability

No data was used for the research described in the article.

Acknowledgement

Afiya Akter Piya thankfully acknowledges the Research cell of Mawlana Bhashani Science and Technology University funded by UGC of Bangladesh (Grant ID: 3631108) as well as department of physics, Mawlana Bhashani Science and Technology University, Tangail-1902.

References

[1] C. Yao, F. Xiang, Z. Xu, Metal oxide nanocage as drug delivery systems for Favipiravir, as an effective drug for the treatment of COVID-19: a computational study, J. Mol. Model. 28 (2022), https://doi.org/10.1007/s00894-022-05054-6.
[2] A.S. Rad, M. Ardjmand, M.R. Esfahani, B. Khodashenas, DFT calculations towards the geometry optimization, electronic structure, infrared spectroscopy and UV–vis analyses of Favipiravir adsorption on the first-row transition metals doped fullerenes; a new strategy for COVID-19 therapy, Spectrochim. Acta - Part A Mol, Biomol. Spectrosc. (2021), https://doi.org/10.1016/j.saa.2020.119082.
[3] N. Yuksel, A. Köse, M.F. Fellah, The supramolecularly complexes of calix[4]arene derivatives toward favipiravir antiviral drug (used to treatment of COVID-19): a DFT study on the geometry optimization, electronic structure and infrared spectroscopy of adsorption and sensing, J. Incl. Phenom. Macrocycl. Chem. 101 (2021) 77–89, https://doi.org/10.1007/s10847-021-01087-1.
[4] C. Chen, Y. Zhang, J. Huang, P. Yin, Z. Cheng, J. Wu, S. Chen, Y. Zhang, B. Chen, M. Lu, Y. Luo, L. Ju, J. Zhang, X. Wang, Favipiravir versus Arbidol for COVID-19: A Randomized Clinical Trial, MedRxiv. (2020) 2020.03.17.20037432.
[5] U. Agrawal, R. Raju, Z.F. Udwadia, Favipiravir: A new and emerging antiviral option in COVID-19, Med. J. Armed Forces India. 76 (2020) 370–376, https://doi.org/10.1016/j.mjafi.2020.08.004.
[6] Y. Furuta, B.B. Gowen, K. Takahashi, K. Shiraki, D.F. Smee, D.L. Barnard, Favipiravir (T-705), a novel viral RNA polymerase inhibitor, Antiviral Res. 100 (2) (2013) 446–454, https://doi.org/10.1016/j.antiviral.2013.09.015.
[7] Z. Jin, L.K. Smith, V.K. Rajwanshi, B. Kim, J. Deval, The Ambiguous Base-Pairing and High Substrate Efficiency of T-705 (Favipiravir) Ribofuranosyl 5′-Triphosphate towards Influenza A Virus Polymerase, PLoS One. 8 (2013), https://doi.org/10.1371/journal.pone.0068347.
[8] Y. Furuta, T. Komeno, T. Nakamura, Favipiravir (T-705), a broad spectrum inhibitor of viral RNA polymerase, Proc. Japan Acad. Ser. B Phys. Biol. Sci. 93 (7) (2017) 449–463, https://doi.org/10.2183/pjab.93.027.
[9] S. Yamazaki, T. Suzuki, M. Sayama, T.-A. Nakada, H. Igari, I. Ishii, Suspected cholestatic liver injury induced by favipiravir in a patient with COVID-19, J. Infect. Chemother. 27 (2) (2021) 390–392, https://doi.org/10.1016/j.jiac.2020.12.021.
[10] M.M. Hasan, A.C. Das, M.R. Hossain, M.K. Hossain, M.A. Hossain, B. Neher, F. Ahmed, The computational quantum mechanical investigation of the functionalized boron nitride nanocage as the smart carriers for favipiravir drug delivery: a DFT and QTAIM analysis, J. Biomol. Struct. Dyn. (2021), https://doi.org/10.1080/07391102.2021.1982776.
[11] Q. Li, Y. Pan, T. Chen, Y. Du, H. Ge, B. Zhang, J. Xie, H. Yu, M. Zhu, Design and mechanistic study of a novel gold nanocluster-based drug delivery system, Nanoscale. (2018), https://doi.org/10.1039/c8nr02189a.
[12] A. Bianco, K. Kostarelos, M. Prato, Applications of carbon nanotubes in drug delivery, Curr. Opin. Chem. Biol. (2005), https://doi.org/10.1016/j.cbpa.2005.10.005.
[13] A.A. Piya, S.U.D. Shamim, M.N. Uddin, K.N. Munny, A. Alam, M.K. Hossain, F. Ahmed, Adsorption behavior of cisplatin anticancer drug on the pristine, Al- and Ga-doped BN nanosheets: A comparative DFT study, Comput. Theor. Chem. (2021), https://doi.org/10.1016/j.comptc.2021.113241.
[14] M. Nishat, M.R. Hossain, M.M. Hasan, M.K. Hossain, M.A. Hossain, F. Ahmed, Interaction of Anagrelide drug molecule on pristine and doped boron nitride nanocages: a DFT, RDG, PCM and QTAIM investigation, J. Biomol. Struct. Dyn. (2022), https://doi.org/10.1080/07391102.2022.2049369.
[15] X. Mei, T. Hu, Y. Wang, X. Weng, R. Liang, M. Wei, Recent advancements in two-dimensional nanomaterials for drug delivery, Wiley Interdiscip. Rev. Nanomed. Nanobiotechnol. 12 (2020), https://doi.org/10.1002/wnan.1596.
[16] İ. Muz, F. Göktaş, M. Kurban, A density functional theory study on favipiravir drug interaction with BN-doped C60 heterofullerene, Phys. E Low-Dimensional Syst. Nanostruct. 135 (2022), https://doi.org/10.1016/j.physe.2021.114950.
[17] H.M. Ghassemi, C.H. Lee, Y.K. Yap, R.S. Yassar, In situ TEM monitoring of thermal decomposition in individual boron nitride nanotubes, JOM. 62 (4) (2010) 69–73, https://doi.org/10.1007/s11837-010-0063-1.
[18] C.R. Dean, A.F. Young, I. Meric, C. Lee, L. Wang, S. Sorgenfrei, K. Watanabe, T. Taniguchi, P. Kim, K.L. Shepard, J. Hone, Boron nitride substrates for high-quality graphene electronics, Nat. Nanotechnol. 5 (10) (2010) 722–726, https://doi.org/10.1038/nnano.2010.172.
[19] A. Pakdel, C. Zhi, Y. Bando, T. Nakayama, D. Golberg, Boron nitride nanosheet coatings with controllable water repellency, ACS Nano. 5 (8) (2011) 6507–6515, https://doi.org/10.1021/nn201838w.
[20] J. Yu, L. Qin, Y. Hao, S. Kuang, X. Bai, Y.M. Chong, W. Zhang, E. Wang, Vertically aligned boron nitride nanosheets: Chemical vapor synthesis, ultraviolet light emission, and superhydrophobicity, ACS Nano. 4 (2010) 414–422, https://doi.org/10.1021/nn901204c.
[21] M.H. Miah, M.R. Hossain, M.S. Islam, T. Ferdous, F. Ahmed, A theoretical study of allopurinol drug sensing by carbon and boron nitride nanostructures: DFT, QTAIM, RDG, NBO and PCM insights, RSC Adv. (2021), https://doi.org/10.1039/d1ra06948a.
[22] T. Ahmed, K. Roy, S. Kakkar, A. Pradhan, A. Ghosh, Interplay of charge transfer and disorder in optoelectronic response in Graphene/hBN/MoS2 van der Waals heterostructures, 2D Mater. 7 (2020), https://doi.org/10.1088/2053-1583/AB771F.
[23] M. Velický, S. Hu, C.R. Woods, P.S. Tóth, V. Zólyomi, A.K. Geim, H.D. Abruña, K. S. Novoselov, R.A.W. Dryfe, Electron Tunneling through Boron Nitride Confirms Marcus-Hush Theory Predictions for Ultramicroelectrodes, ACS Nano. 14 (1) (2020) 993–1002.
[24] G.-H. Lee, Y.-J. Yu, X.u. Cui, N. Petrone, C.-H. Lee, M.S. Choi, D.-Y. Lee, C. Lee, W. J. Yoo, K. Watanabe, T. Taniguchi, C. Nuckolls, P. Kim, J. Hone, Flexible and transparent MoS2 field-effect transistors on hexagonal boron nitride-graphene heterostructures, ACS Nano. 7 (9) (2013) 7931–7936, https://doi.org/10.1021/nn402954e.
[25] K. Zhang, Y. Feng, F. Wang, Z. Yang, J. Wang, Two dimensional hexagonal boron nitride (2D-hBN): Synthesis, properties and applications, J. Mater. Chem. C. 5 (46) (2017) 11992–12022.
[26] D. Pacíl, J.C. Meyer, Ç. Girit, A. Zettl, The two-dimensional phase of boron nitride: Few-atomic-layer sheets and suspended membranes, Appl. Phys. Lett. 92 (2008), https://doi.org/10.1063/1.2903702.
[27] L.H. Li, Y. Chen, G. Behan, H. Zhang, M. Petravic, A.M. Glushenkov, Large-scale mechanical peeling of boron nitride nanosheets by low-energy ball milling, J. Mater. Chem. 21 (2011) 11862–11866, https://doi.org/10.1039/c1jm11192b.
[28] C. Jin, F. Lin, K. Suenaga, S. Iijima, Fabrication of a freestanding boron nitride single layer and Its defect assignments, Phys. Rev. Lett. 102 (2009), https://doi.org/10.1103/PhysRevLett.102.195505.
[29] A. Nag, K. Raidongia, K.P.S.S. Hembram, R. Datta, U.V. Waghmare, C.N.R. Rao, Graphene analogues of BN: Novel synthesis and properties, ACS Nano. 4 (2010) 1539–1544, https://doi.org/10.1021/nn9018762.
[30] S.M. Sharker, Hexagonal boron nitrides (White graphene): A promising method for cancer drug delivery, Int. J. Nanomedicine. 14 (2019) 9983–9993, https://doi.org/10.2147/IJN.S205095.
[31] M. Vatanparast, Z. Shariatinia, Hexagonal boron nitride nanosheet as novel drug delivery system for anticancer drugs: Insights from DFT calculations and molecular dynamics simulations, J. Mol. Graph. Model. (2019), https://doi.org/10.1016/j.jmgm.2019.02.012.
[32] T.A. Hilder, N. Gaston, Interaction of Boron Nitride Nanosheets with Model Cell Membranes, ChemPhysChem. 17 (11) (2016) 1573–1578, https://doi.org/10.1002/cphc.201600165.
[33] S.A. Nazari, F. Farzad, A. Haghi, A. Bina, Surface functionalization of boron nitride nanosheet with folic acid: Toward an enhancement in Doxorubicin anticancer drug

loading performance, J. Mol. Graph. Model. 109 (2021), https://doi.org/10.1016/j.jmgm.2021.108041.
[34] Y. Cao, M. Kamel, K. Mohammadifard, A. Heshmati J. M, M.R. Poor Heravi, A. Ghaffar Ebadi, Probing and comparison of graphene, boron nitride and boron carbide nanosheets for Flutamide adsorption: A DFT computational study, J. Mol. Liq. 343 (2021). 10.1016/j.molliq.2021.117487.
[35] M.R. Hossain, M.M. Hasan, N.E. Ashrafi, H. Rahman, M.S. Rahman, F. Ahmed, T. Ferdous, M.A. Hossain, Adsorption behaviour of metronidazole drug molecule on the surface of hydrogenated graphene, boron nitride and boron carbide nanosheets in gaseous and aqueous medium: A comparative DFT and QTAIM insight, Phys. E Low-Dimensional Syst. Nanostructures. (2021), https://doi.org/10.1016/j.physe.2020.114483.
[36] M. Doust Mohammadi, H.Y. Abdullah, V. Kalamse, A. Chaudhari, Bromochlorodifluoromethane interaction with pristine and doped BN nanosheets: A DFT study, J. Environ Chem. Eng. 10 (5) (2022) 108367, https://doi.org/10.1016/j.jece:2022.108367.
[37] M. Doust Mohammadi, H.Y. Abdullah, Theoretical study of the adsorption of amantadine on pristine, Al-, Ga-, P-, and As-doped boron nitride nanosheets: a PBC-DFT, NBO, and QTAIM study, Theor. Chem. Acc. (2020), https://doi.org/10.1007/s00214-020-02672-2.
[38] T. Ahmed, M. Aminur Rahman, R. Islam, A. Akter Piya, S. Ud Daula Shamim, Unravelling the adsorption performance of BN, AlN, GaN and InN 2D nanosheets towards the ciclopirox, 5-fluorouracil and nitrosourea for anticancer drug delivery motive: A DFT-D with QTAIM, PCM and COSMO investigations, Comput. Theor. Chem. 1214 (2022) 113797. 10.1016/J.COMPTC.2022.113797.
[39] J.P. Perdew, K. Burke, M. Ernzerhof, Generalized gradient approximation made simple, Phys. Rev. Lett. 77 (18) (1996) 3865–3868, https://doi.org/10.1103/PhysRevLett.77.3865.
[40] B. Delley, Hardness conserving semilocal pseudopotentials, Phys. Rev. B - Condens. Matter Mater. Phys. (2002), https://doi.org/10.1103/PhysRevB.66.155125.
[41] S.U.D. Shamim, M.K. Hossain, S.M. Hasan, A.A. Piya, M.S. Rahman, M.A. Hossain, F. Ahmed, Understanding Na-ion adsorption in nitrogen doped graphene oxide anode for rechargeable sodium ion batteries, Appl. Surf. Sci. 579 (2022), 152147, https://doi.org/10.1016/j.apsusc.2021.152147.
[42] Z.J. Sui, Y.A. Zhu, P. Li, X.G. Zhou, D. Chen, Kinetics of catalytic dehydrogenation of propane over Pt-based catalysts, Adv. Chem. Eng. 44 (2014) 60–125, https://doi.org/10.1016/B978-0-12-419974-3.00002-6.
[43] J. Mawwa, S.U.D. Shamim, S. Khanom, M.K. Hossain, F. Ahmed, In-plane graphene/boron nitride heterostructures and their potential application as toxic gas sensors, RSC Adv. 11 (52) (2021) 32810–32823.
[44] C. Xiao, K. Ma, G. Cai, X. Zhang, E. Vessally, Borophene as an electronic sensor for metronidazole drug: A computational study, J. Mol. Graph. Model. 96 (2020), https://doi.org/10.1016/j.jmgm.2020.107539.
[45] R.G. Pearson, Chemical hardness and density functional theory, J. Chem. Sci. (2005), https://doi.org/10.1007/BF02708340.
[46] P.J. Hay, W.R. Wadt, Ab initio effective core potentials for molecular calculations. Potentials for the transition metal atoms Sc to Hg, J. Chem. Phys. 82 (1) (1985) 270–283, https://doi.org/10.1063/1.448799.
[47] S.U.D. Shamim, T. Hussain, M.R. Hossian, M.K. Hossain, F. Ahmed, T. Ferdous, M. A. Hossain, A DFT study on the geometrical structures, electronic, and spectroscopic properties of inverse sandwich monocyclic boron nanoclusters ConBm (n = 1.2; m = 6–8), J. Mol. Model. 26 (2020), https://doi.org/10.1007/s00894-020-04419-z.
[48] D. Farmanzadeh, M. Keyhanian, Computational assessment on the interaction of amantadine drug with B12N12 and Zn12O12 nanocages and improvement in adsorption behaviors by impurity Al doping, Theor. Chem. Acc. (2019), https://doi.org/10.1007/s00214-018-2400-3.
[49] M. Rakib Hossain, M. Mehade Hasan, S. Ud Daula Shamim, T. Ferdous, M. Abul Hossain, F. Ahmed, First-principles study of the adsorption of chlormethine anticancer drug on C24, B12N12 and B12C6N6 nanocages, Comput. Theor. Chem. (2021). 10.1016/j.comptc.2021.113156.
[50] S. Sadeghzadeh, M.M. Khatibi, Vibrational modes and frequencies of borophene in comparison with graphene nanosheets, Superlattices and Microstructures 117 (2018) 271–282.
[51] H. Zhao, Q. Zhu, C. Zhang, J. Li, M. Wei, Y. Qin, G. Chen, K. Wang, J. Yu, Z. Wu, X. Chen, G. Wang, Tocilizumab combined with favipiravir in the treatment of COVID-19: A multicenter trial in a small sample size, Biomed. Pharmacother. (2021), https://doi.org/10.1016/j.biopha.2020.110825.
[52] İ. Muz, F. Göktaş, M. Kurban, A density functional theory study on favipiravir drug interaction with BN-doped C60 heterofullerene, Phys. E Low-Dimensional Syst. Nanostruct. (2022), https://doi.org/10.1016/j.physe.2021.114950.
[53] F. Shi, Z. Li, L. Kong, Y. Xie, T. Zhang, W. Xu, Synthesis and crystal structure of 6-fluoro-3-hydroxypyrazine-2-carboxamide, Drug Discov. Ther. (2014), https://doi.org/10.5582/ddt.2014.01028.
[54] M.G. Ahangari, A.H. Mashhadzadeh, M. Fathalian, A. Dadrasi, Y. Rostamiyan, A. Mallahi, Effect of various defects on mechanical and electronic properties of zinc-oxide graphene-like structure: A DFT study, Vacuum. (2019), https://doi.org/10.1016/j.vacuum.2019.04.003.
[55] A. Ahmadi Peyghan, N.L. Hadipour, Z. Bagheri, Effects of Al doping and double-antisite defect on the adsorption of HCN on a BC2N nanotube: Density functional theory studies, J. Phys. Chem. C. (2013), https://doi.org/10.1021/jp312503h.
[56] L. Li, J. Zhao, Defected boron nitride nanosheet as an electronic sensor for 4-aminophenol: A density functional theory study, J. Mol. Liq. (2020), https://doi.org/10.1016/j.molliq.2020.112926.
[57] S.U.D. Shamim, M.H. Miah, M.R. Hossain, M.M. Hasan, M.K. Hossain, M. A. Hossain, F. Ahmed, Theoretical investigation of emodin conjugated doped B12N12 nanocage by means of DFT, QTAIM and PCM analysis, Phys. E Low-Dimensional Syst. Nanostructures. 136 (2022), 115027, https://doi.org/10.1016/j.physe.2021.115027.
[58] S. Dushman, Electron Emission from Metals as a Function of Temperature, Phys. Rev. 21 (6) (1923) 623–636.
[59] S.U.D. Shamim, D. Roy, S. Alam, A.A. Piya, M.S. Rahman, M.K. Hossain, F. Ahmed, Doubly doped graphene as gas sensing materials for oxygen-containing gas molecules: A first-principles investigation, Appl. Surf. Sci. 596 (2022), 153603, https://doi.org/10.1016/j.apsusc.2022.153603.
[60] S.N. Ema, M.A. Khaleque, A. Ghosh, A.A. Piya, U. Habiba, S.U.D. Shamim, Surface adsorption of nitrosourea on pristine and doped (Al, Ga and In) boron nitride nanosheets as anticancer drug carriers: The DFT and COSMO insights, RSC Adv. 11 (58) (2021) 36866–36883.
[61] M.R. Hossain, M.M. Hasan, M. Nishat, F. Noor-E-Ashrafi, T. Ahmed, M.A. H. Ferdous, DFT and QTAIM investigations of the adsorption of chlormethine anticancer drug on the exterior surface of pristine and transition metal functionalized boron nitride fullerene, J. Mol. Liq. (2021), https://doi.org/10.1016/j.molliq.2020.114627.